Hindawi Publishing Corporation
Journal of Sensors
Article ID 641798

Research Article

Impact of Topography and Tidal Height on ALOS PALSAR Polarimetric Measurements to Estimate Aboveground Biomass of Mangrove Forest in Indonesia

S. Darmawan,[1,2,3] W. Takeuchi,[1] Y. Vetrita,[4] K. Wikantika,[2] and D. K. Sari[3]

[1] *Institute of Industrial Science, University of Tokyo, Tokyo 153-8505, Japan*
[2] *Center for Remote Sensing, Institut Teknologi Bandung (ITB), Bandung 40132, Indonesia*
[3] *Institut Teknologi Nasional (ITENAS), Bandung 40124, Indonesia*
[4] *Indonesian National Institute of Aeronautics and Space (LAPAN), Jakarta 13710, Indonesia*

Correspondence should be addressed to S. Darmawan; soni_darmawan@yahoo.com

Received 7 January 2015; Accepted 24 April 2015

Academic Editor: Jian Yang

This study is focused on investigating the impact of topography and tidal height on ALOS PALSAR polarimetric measurements on HH and HV for estimating aboveground biomass (AGB) of mangrove forest in Indonesia. We used multitemporal ALOS PALSAR polarimetric measurement that covered mangrove zone in Banyuasin, Cilacap, and Teluk Bintuni and also collected tidal height data within the same acquisition date with multitemporal ALOS PALSAR polarimetric measurement. We analyzed the distribution of flooding and nonflooding areas based on tidal height and SRTM topography data, created three profiles as region of interest (ROI), and got characteristics of backscatter value on HH and HV with different tidal height. The result of this study showed backscatter of the open mangrove zones during high tide with HH value less than −20 dB and HV value less than −25 dB whereas during low tide it showed an HH value around −20 to −10 dB and HV value around −25 to −10 dB. Backscatter of the middle mangrove zones at Cilacap, with low and flat topography, showed a deviation of backscatter on HV value of 1.6 dB. Finally, the average AGB of mangrove forest in Indonesia was estimated based on ALOS PALSAR polarimetric measurements.

1. Introduction

The term of "mangrove" is used to define both the plants that populate the tidal forests and to describe the community itself [1–3]. Mangrove forests can be found along ocean coastlines throughout the tropics and provide important products and services [4]. They are also among the most intense coastal carbon sinks in the world and play a growing and central role in the global carbon cycle [5]. According to Donato et al. [6] mangroves have five times larger number of total carbon storage per unit area basis on average than those typically observed in temperate, boreal, and tropical terrestrial forests. This suggests that mangroves play an important role in global climate change management. In order to gain and build a solid understanding of the global carbon budget and ultimately the effects of diminishing mangrove forests on climate change, it is crucial to obtain an assessment and quantification of the spatial distribution of mangrove forest biomass. Indonesia has the largest mangroves area in the world, covering an area around 3.5 million ha or around 17%–23% of all mangrove areas in the world [7]. The loss of more than 50% of global mangrove area in recent years suggested the growing importance of mapping and monitoring biomass of mangrove forest. However, conducting field survey for mangrove biomass and its productivity in Indonesia region is proven to be very difficult due to muddy soil condition, heavy weight of the wood [8], the vast area to cover, and tidal influences.

Remote sensing has been widely proven to be essential in monitoring and mapping highly threatened mangrove ecosystems. Tropical and subtropical coastal mangroves are among the most threatened and vulnerable ecosystems worldwide [4]. According to Henderson and Lewis [9], although sensors in the optical range of the electromagnetic spectrum have received the greatest attention, considerable effort has also been focused on the use of imaging radars. There are many reasons to use radar to monitor and map mangrove ecosystems. As radar operates in the microwave portion of the spectrum, it offers complementary and supplementary data to sensors operating in the optical and thermal bands. At the same time, it also patently provides unique data. Radar backscatter is sensitive to dielectric properties (soil and vegetation moisture content) and geometric (surface roughness) attributes of the imaged surface. In many areas of the world (e.g., cloud-covered and/or low-light regions of the Earth) imaging radar is the only sensor that can provide consistent, periodic data in reliable manner. Optical and thermal systems are also limited by their inability to penetrate vegetation canopies whereas radar systems can, to some degree, provide subcanopy information.

The launch of the Japanese Space Exploration Agency's (JAXA) Advanced Land Observing Satellite (ALOS) Phased Arrayed L-band SAR (PALSAR) in 2006 therefore represented a milestone in the global observation, characterization, mapping, and monitoring of mangroves largely, because these provide more information on the three-dimensional structure and biomass of woody vegetation, as well as the presence and the extent of (primarily tidal) inundation. As data can be days or night regardless of weather conditions, mangroves can be observed more frequently, even in regions with prevalent cloud cover. ALOS-PALSAR penetrates through the foliage and interacts primarily with the woody components of vegetation. Horizontally transmitted waves are either depolarized through volume scattering by branches in the canopy, with a proportion of vertically polarized microwaves returning to the sensor, or penetrate through the canopy and interact with the trunks, returning primarily through double bounce scattering as a horizontally polarized wave [10]. Longer L-band microwaves have a greater likelihood of penetrating the foliage and small branches at the upper canopies of the forest and interacting with woody trunk and larger branch components as well as the underlying surface [11, 12]. L-band SAR (1.3 GHz, 23.5 cm) generally provides greater penetration of forest canopies than does the shorter C-band (5.3 GHz, 5.7 cm) because the wavelength is longer than leaf sizes within the forest canopy [13–17]. Thus, ALOS PALSAR is proven to be potential to estimate aboveground biomass of mangrove forest [8, 10, 18, 19]. The modeling approach treats tree canopy, tree trunks, and ground surface as layered scattering media that scatter and attenuate the incoming microwave energy. The model has four components: surface backscatter (σ_s°), canopy volume scattering (σ_c°), multiple path interactions of canopy-ground (σ_m°), and double bounce trunk-ground interactions (σ_d°). Incoherent summation of the components results in total backscatter (σ_t°) with the algorithms as shown in the following [14]:

$$\sigma_t^\circ = \sigma_s^\circ + \sigma_c^\circ + \sigma_m^\circ + \sigma_d^\circ. \quad (1)$$

The sensitivity of the backscatter to forest parameters and the saturation level is rather sites-dependent, since forest structure influences the relative contribution of the scattering mechanism [12, 19, 20]. In addition, the individual contribution to the total forest backscatter is also dependent on environmental conditions (i.e., weather conditions, moisture conditions, and weather dynamics) which can affect the dielectric properties of the vegetation and ground surface. The interactions between the radiation and the plant's internal properties (e.g., moisture content influencing the dielectric constant of a material and cell structure) and external components (e.g., size, geometry, and orientation of leaves, trunks, branches, and aerials or stilt roots) also result in a specific backscatter signal [4, 19]. The unique location of mangroves at the zones of transition between terrestrial and marine ecosystem that occurs in tidal forest and the capability of L-band to penetrate until underlying surface lead to a question of the probable impact of tidal height on characteristics of ALOS PALSAR measurement. Hence, the objective of this research is to investigate the impact of topography and tidal height on characteristics of HH and HV derived from ALOS PALSAR measurements for the estimation of aboveground biomass of mangrove forest.

2. Study Area

Indonesia is a country in Southeast Asia that is located on 6° N–11° S and 95° E–141° E, between the Asian and Australian continents, and between the Pacific and Indian Oceans. Indonesia has approximately 17,500 islands and is considered to be the largest archipelagic country in the world. Generally mangroves can be found throughout the Indonesian archipelago, with the largest mangrove area of around 1.3 million ha (38%) found in Papua, around 978 thousand ha (28%) in Kalimantan, and 673 thousand ha (19%) in Sumatera [7]. Indonesian mangrove area can be categorized into four zones [7]. The first is the open zones which sit at the forefront of the sea and the majority of its mangrove types are *Sonneratia alba*. The second is middle zones, which sit behind the open zones and the majority of its mangrove types are *Rhizophora*. The third is payau zone, located along the river, and the majority of its mangrove types are *Nypa* or *Sonneratia*. The fourth is land zone, located behind middle zones and payau zone, and is inhabited by a larger variety of plants species compared to the other three zones.

The area of study for this investigation of topography and tidal height impacts on ALOS PALSAR polarimetric measurements of HH and HV is focused on Banyuasin, South Sumatera (104.464 E, −1.897 N), Cilacap Central Java (108.832 E, −7.679 N) and Teluk Bintuni Papua (133.470 E, −2.525 N). The locations are specifically chosen for their representativeness of all mangrove forest in Indonesia. Profiling as samples of regions of interest (ROIs) was created in each study area. Each study area has three ROIs (e.g., Banyuasin: d1, d2, d3; Cilacap: k1, k2, k3; Teluk bintuni: q1, q2, q3) which can be seen in Figures 1(B), 1(C), and 1(D). The estimation for aboveground biomass is focused on twenty sites of mangrove zones in Indonesia as follows: (a) Langsa, Aceh, (b) Bengkalis, Riau, (c) Indragiri Hilir, Riau, (d) Banyuasin, South Sumatera, (e) Pontianak, West Kalimantan, (f) Kotabaru, South Kalimantan, (g) Kutai Kartanegara, East Kalimantan, (h) Berau, East Kalimantan, (i) Nunukan, East Kalimantan, (j) Subang, West Java, (k) Cilacap, Central Java, (l) Badung, Bali (m)

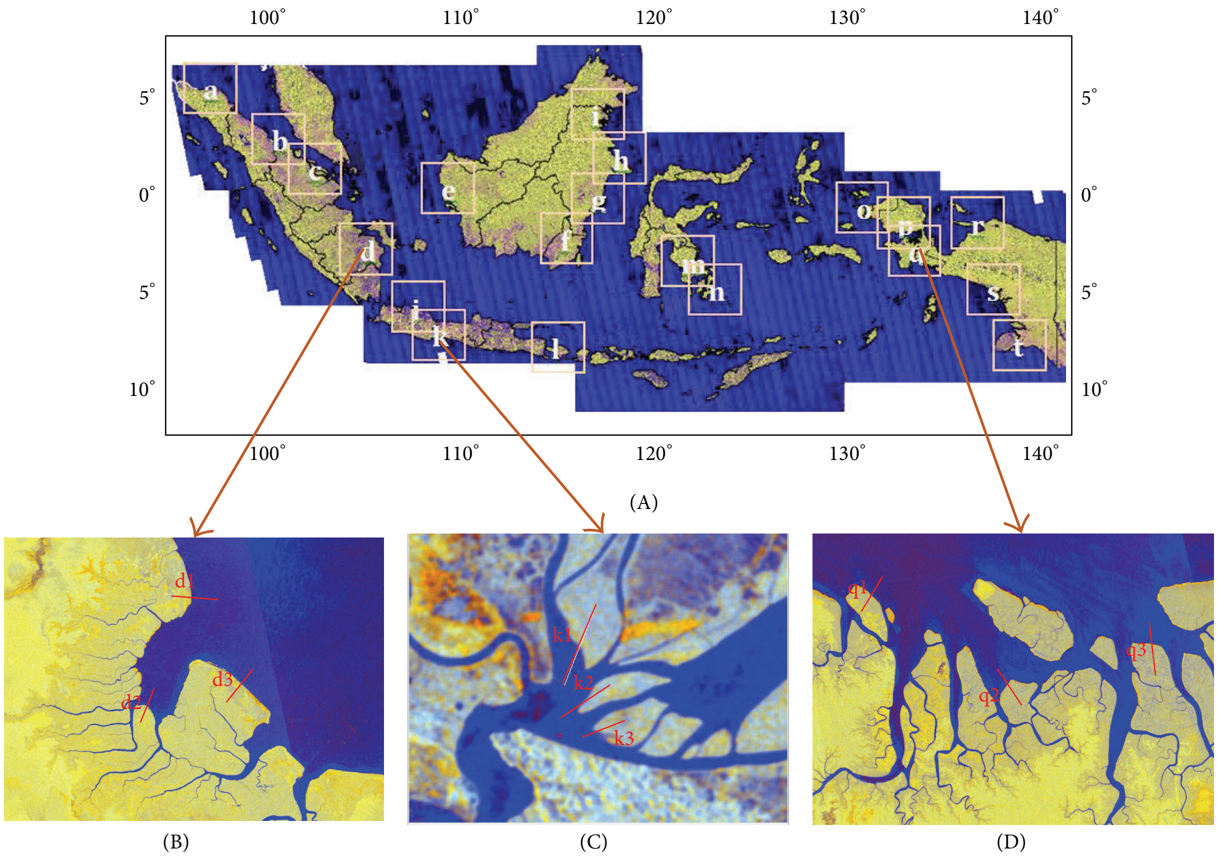

Figure 1: Study areas are twenty sites for estimation AGB in Indonesia (A) and ROI in Banyuasin, South Sumatera (B), Cilacap, Central Java (C), and Teluk Bintuni, Papua (D) for investigation impact of topography and tidal height.

Bombana, Southeast Sulawesi (n) Muna, Southeast Sulawesi, (o) Sorong, West Papua, (p) Teluk Bintuni, Papua, (q) Teluk Bintuni, Papua, (r) Waropen, Papua, (s) Asmat, Papua, and (t) Merauke Papua. Their location is shown in Figure 1(A).

3. Methodology

This study collected ALOS PALSAR data, ALOS PALSAR mosaics data, Shuttle Radar Topographic Missions (SRTM) data, and tidal height data. Preprocessing is focused on converting digital number to normalize radar cross sections (NRCS) and filtering of ALOS PALSAR data, profiling of ALOS PALSAR data and calculation of statistic, and calculation of aboveground biomass.

3.1. Data Used in This Study. We collected primary data of dual polarization ALOS PALSAR L-band HH and HV with spatial resolution of 12.5 m. Product ID H1.5 GUA with radiometric and geometric corrections are performed based on the map projection, fine mode was selected for pixel spacing, and the calculation of latitudes and longitudes in the product omitted the altitude. All data were acquired in fine beams dual modes at a viewing angle of 34.3 and delivered in single-look complex (SLC) as the normalized backscattering coefficient in slant-range geometry by JAXA. ALOS PALSAR data collected in this study was described on Table 1.

We also used dual polarization ALOS PALSAR L-band HH and HV spatial resolution 50 m orthorectified mosaic product in 2008 from Kyoto and Carbon Initiative.

For secondary data, we collected topography elevation data derived from SRTM which have spatial resolution approximately 90 meters and were processed by NASA and USGS. The data was projected in a Geographic (Lat/Long) projection, with the WGS84 horizontal datum and the EGM96 vertical datum. Another secondary data were sea level measurement data from http://www.ioc-sealevelmonitoring.org/. Tidal height data on mangrove zones in Cilacap is shown in Figure 2 as an example. The site has been expanded to a global station monitoring service for measuring of real times sea level that are part of Intergovernmental Oceanographic Commission (IOC) of UNESCO programs. According to Figure 2, the tidal height of ALOS PALSAR measurement at 30-04-2008 15:33:49.697, 09-05-2008 02:50:03.551, and 15-06-2008 15:33:31.460 is around −0.4 meters, 1.0 meter, and −0.2 meters, respectively.

3.2. Preprocessing and Biomass Estimation. Preprocessing was focused on converting digital number (DN) into normalize radar cross sections (NRCS) and filtering of ALOS PALSAR data. The conversion of HH (DN_{HH}) and HV (DN_{HV})

Table 1: ALOS PALSAR data was used on study.

Scene ID	Nadir angle	Polarizations	Acquisition date on scene center	Location
ALPSRP1 22177140	34.3	HH and HV	10052008-15:48:07.749	Banyuasin South Sumatera
ALPSRP1 28887140	34.3	HH and HV	25062008-15:47:35.329	
ALPSRP1 20717030	34.3	HH and HV	30042008-15:33:49.697	Cilacap West Java
ALPSRP1 21953770	34.3	HH and HV	09052008-02:50:03.551	
ALPSRP1 27427030	34.3	HH and HV	15062008-15:33:31.460	
ALPSRP1 29167130	34.3	HH and HV	27062008-13:52:53.001	Teluk Bintuni Papua
ALPSRP1 42587130	34.3	HH and HV	27092008-13:51:32.107	

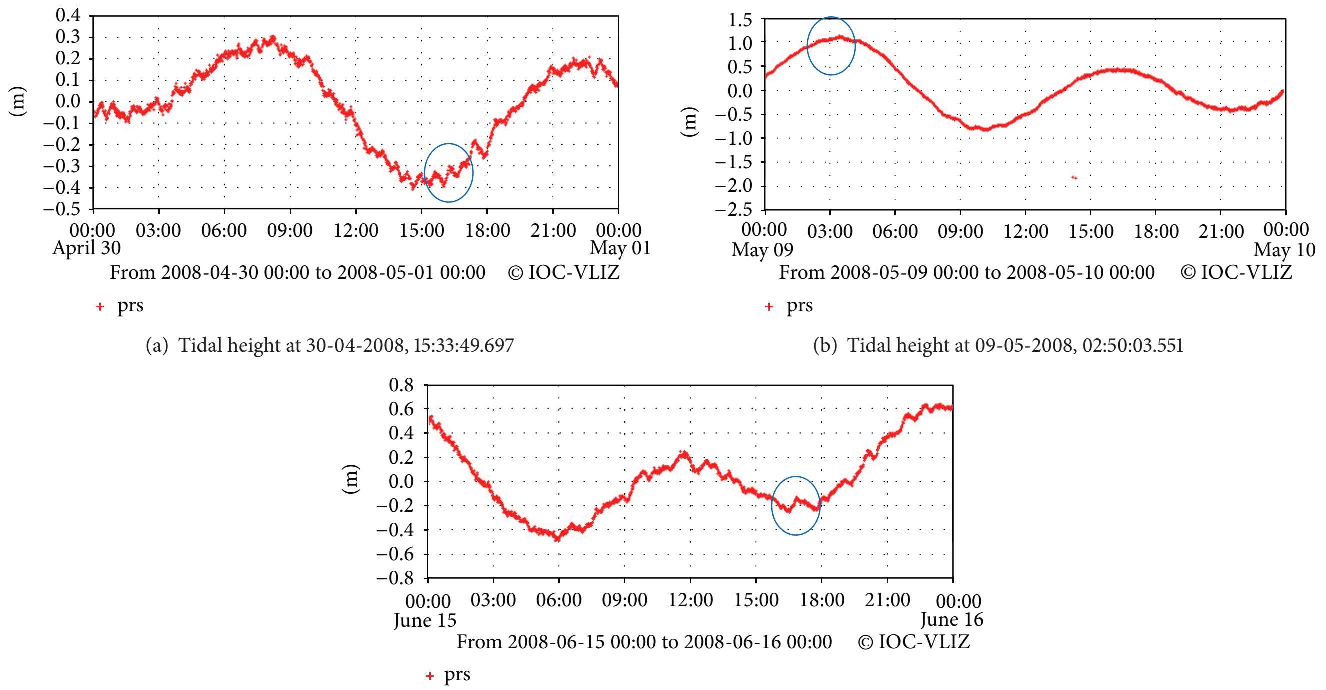

(a) Tidal height at 30-04-2008, 15:33:49.697

(b) Tidal height at 09-05-2008, 02:50:03.551

(c) Tidal height at 15-06-2008, 15:33:31.460

Figure 2: Tidal height data corresponding to the same acquisition date with multitemporal ALOS PALSAR polarimetric measurements in Cilacap area (source: http://www.ioc-sealevelmonitoring.org/).

backscatter intensities into NRCS (i.e., $\sigma^{\circ}{}_{\mathrm{HH}}$ and $\sigma^{\circ}{}_{\mathrm{HV}}$) was based on Shimada et al. [21], while for the reduction of speckle noise we used frost filtering with windows size 6 × 6. The conversion of DN into NRCS used the following equations:

$$\sigma^{\circ}{}_{\mathrm{HH}} = 10\log_{10}\left(\mathrm{DN}^{2}{}_{\mathrm{HH}}\right) - 83.2,$$
$$\sigma^{\circ}{}_{\mathrm{HV}} = 10\log_{10}\left(\mathrm{DN}^{2}{}_{\mathrm{Hv}}\right) - 83.2. \quad (2)$$

The regions of interest (ROIs) of mangrove forest were determined based on land cover maps from Indonesian Ministry of Forestry and Indonesian base map from Badan Informasi Geospasial (BIG). ROI has the shape of line profiling with length of around 80 to 420 pixels. There were three ROIs of mangrove forest from ALOS PALSAR and SRTM data for each study area, all with calculated means and standard deviations. Several study [8, 10, 19] has established empirical relationships between L-band backscatter and aboveground

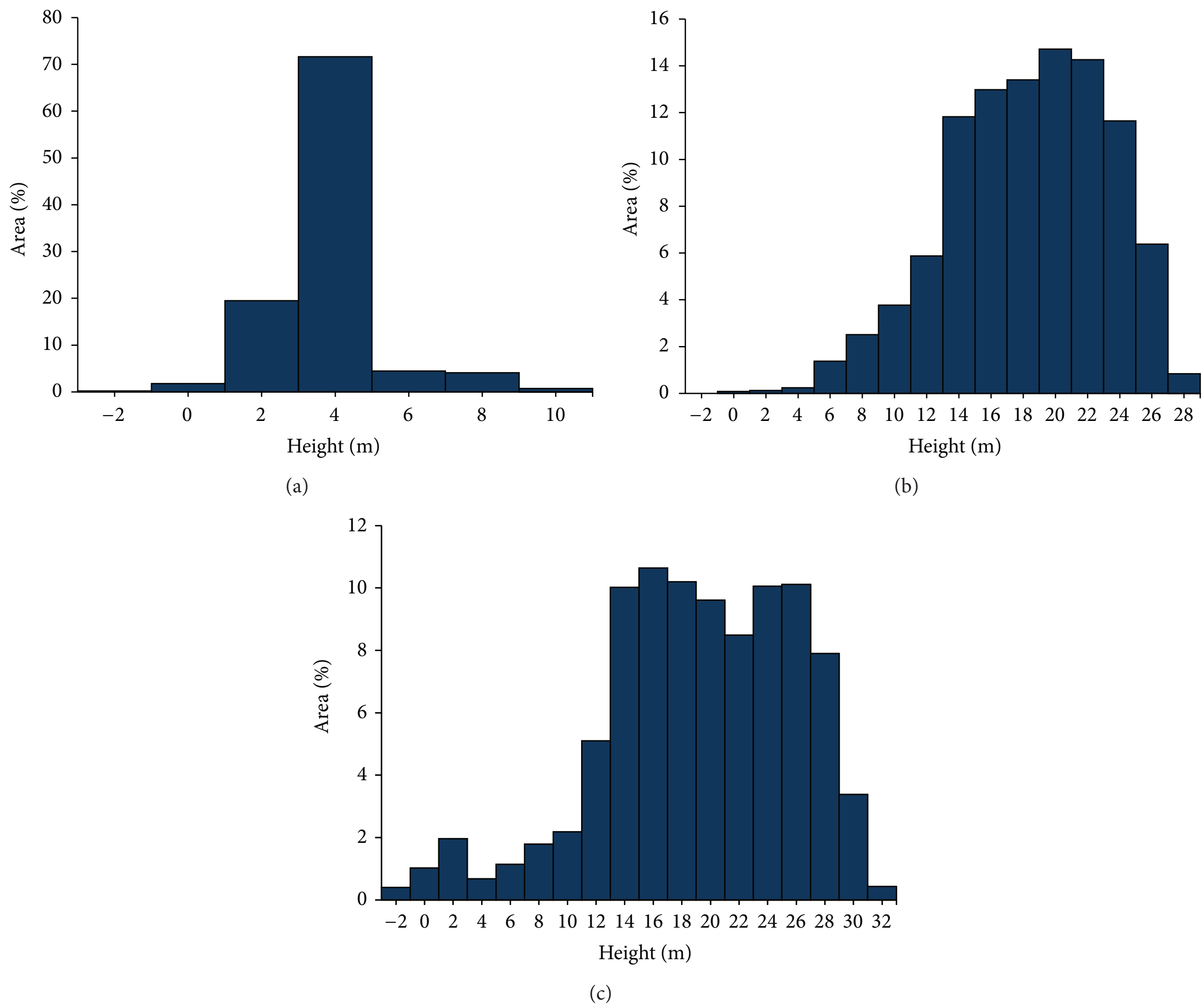

Figure 3: Level of topography at study area: (a) Cilacap, West Java, (b) Banyuasin, South Sumatera, and (c) Teluk Bintuni, Papua.

biomass (AGB) of mangrove forest. For this study, we calculated the aboveground biomass with the following equations [8]:

$$\begin{gathered} \mathrm{HH}\left(\sigma^{\circ}\right)=3.6 \ln (\text{tree height})-23.7, \\ \mathrm{HV}\left(\sigma^{\circ}\right)=4.4 \ln (\text{tree height})-24.9, \\ \text{tree height}=2.8 \ln (\mathrm{DBH})+23.7, \\ \mathrm{AGB}=0.25\, \mathrm{DBH}^{2.46}. \end{gathered} \tag{3}$$

According to Lucas et al. [10], however, an understanding of microwave interaction with the forest volume has proven to be difficult to achieve using empirical relationships with SAR data due to inherent relationships between these components. The retrieval of component biomass was also more difficult in forests above the level of saturation (herein referred to as high biomass forests) compared with those below the level of saturation (low biomass forests), as greater attenuation by the crown volume reduces the diversity of scattering mechanisms between components and the ground surface. Hence, less information on the forest biomass and structure (and therefore species, growth stage, and form) can be extracted. However, by considering the scattering mechanisms operating within low and high forests, separately, L-band SAR data can be better interpreted.

4. Results and Discussion

4.1. Flooding and Nonflooding on Mangrove Zones. Mangrove forests occupy zones of transition between terrestrial and marine ecosystems determined by the cumulative and complex interaction between hydrology, landscape positions, sediment dynamics, storm-driven processes, sea level change, and subsidence [22]. Tidal flooding patterns are important aspects of mangrove forest [23, 24]. Tidal flooding and surface drainage pattern have often been used to describe mangrove species zonation [25]. Tidal flooding distribution depends on level of topography and tidal height on study area. The level of topography at the study areas derived from SRTM is shown in Figure 3.

According to Figure 3, the dominant level of topography at Cilacap is 4 meters and less, covering around 90% of its

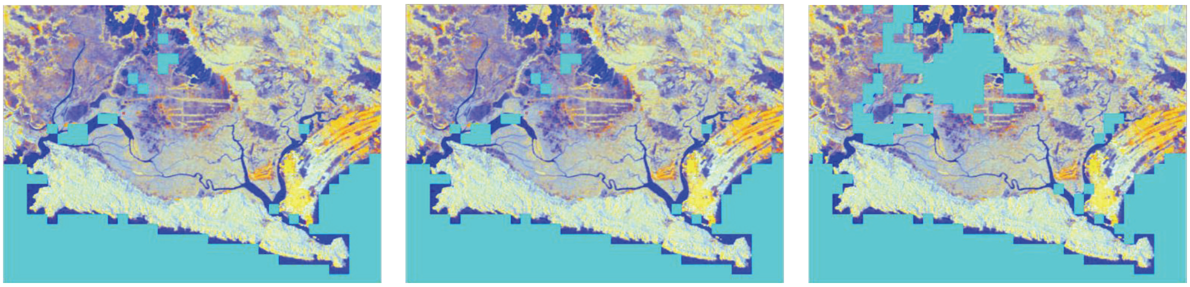

(a) (b) (c)

Figure 4: Illustration of distribution of flooding and nonflooding at mangrove zone from ALOS PALSAR composite and cyan colors is water (a) tidal height on −0.4 meters, (b) tidal height on −0.2, and (c) tidal height on 1.0 meter.

total area. Different topographical characteristics are shown for Banyuasin and Teluk Bintuni, where both tend to have varieties of topography at higher height, leaving only around 10% of their total area with the height of 4 meters and less. It means that Cilacap area has relatively low and flat topography, while Banyuasin and Teluk Bintuni are situated at higher topography and have a wider variety of topographical features. It is worth noting that SRTM has a limited accuracy around 5 to 10 meters [26] for topography analysis on mangrove forest. But since more accurate topographical data was impossible to obtain during the study, that is, data derived from surveys terrestrial, photogrammetry, or LIDAR, we believe that this SRTM topography data was sufficient to provide general descriptions for the level of topography at the selected study areas.

The average annual tidal height on the study area is around −1.5 to 1.5 meters, and variances of tidal height will cause variances of flood areas to occur at mangrove zones. However, the size and the spatial distribution of flood areas at mangrove zones were also determined by the level of topography in study areas. Figure 4 illustrates the effect of the level of topography and tidal height to the distribution of flood areas in Cilacap.

Figure 4 shows how various tidal height caused differences in the size and spatial distribution of flood areas. The higher the tidal height is, the larger the areas of flood occurred. With the cyan pixel representing water, the map showed that tidal height of 1 meter can cause much larger areas of flood compared to those caused by much less tidal height. If the pattern continued, a tidal height of 4 meters shall have a very high probability to drown the entire area of mangrove zones due to the relatively low and flat topography of the area. And if we considered the zoning of mangrove areas [7], we can safely assume that the open zones experience stronger impact tidal height than middle zones or land zones. However, it is worth noting that the spatial distribution of flooding on mangrove zones was not solely determined by tidal height and topography but also by rainfall [25], surface roughness [27], vegetation density [23], and human activity.

4.2. Impacts of Flooding on Backscatter Characteristics. Aside from using tidal flooding and surface drainage pattern to describe mangrove species zonation, tidal flooding may have influence on ALOS PALSAR polarimetric measurement on HH and HV. We have created three ROIs in Banyuasin (d1, d2, d3), Cilacap (k1, k2, k3), and Teluk Bintuni (q1, q2, q3) with multitemporal ALOS PALSAR polarimetric measurement on HH and HV. Multitemporal ALOS PALSAR polarimetric measurement suggests different tidal height, and our next discussions shall focus on the impact of those differences to various zones of mangrove in Banyuasin, Cilacap, and Teluk Bintuni. Each study area has unique characteristics of backscatter value on HH and HV that depend on wavelengths, polarization, incident angle, and temporal data [25], as well as environment (e.g., tidal height, topography, and landscape) and mangrove structure, and will be described exclusively in each section.

4.2.1. Case Study in Banyuasin South Sumatera. We used two ALOS PALSAR polarimetric measurements on HH and HV which covers mangrove forest at Banyuasin South Sumatera. The first acquisition date was on 10-05-2008 at 15.48:07.749, while the second acquisition date was on 25-06-2008 at 15:47:35.329. Each acquisition date has differences in tidal height, whereas tidal height on the first acquisition date is higher than that of the second. SRTM data of topography level in Banyuasin showed that most of the study area has high topography, with topography of less than 4 meters only covering 10% of total area.

Figure 5 shows the impact of tidal height on ALOS PALSAR polarimetric measurement on HH and HV based on profiling of ROI with length of 420 pixels. The number 0 (zero) on the axis "distance on pixel" serves as a starting point for water areas. The water area (distance on pixel 0–60 at d1) shows a majority of backscatter value of less than −20 dB on HH and HV, indicating the specular reflection of ALOS PALSAR radiation which produces small backscatter value. The open zone has different backscatter patterns between the two acquisition dates of 10-05-2008 and 25-06-2008, which might be caused by different tidal height. The measurement on 10-05-2008 shows lower tides, creating a nonflooding condition at the open zone. On the nonflooding areas, ALOS PALSAR penetrated the mangrove areas and dry surface so ALOS PALSAR radiation has multiple and double bounce reflection which produce backscatter value on HH and HV around −20 dB to −10 dB. Different conditions showed on

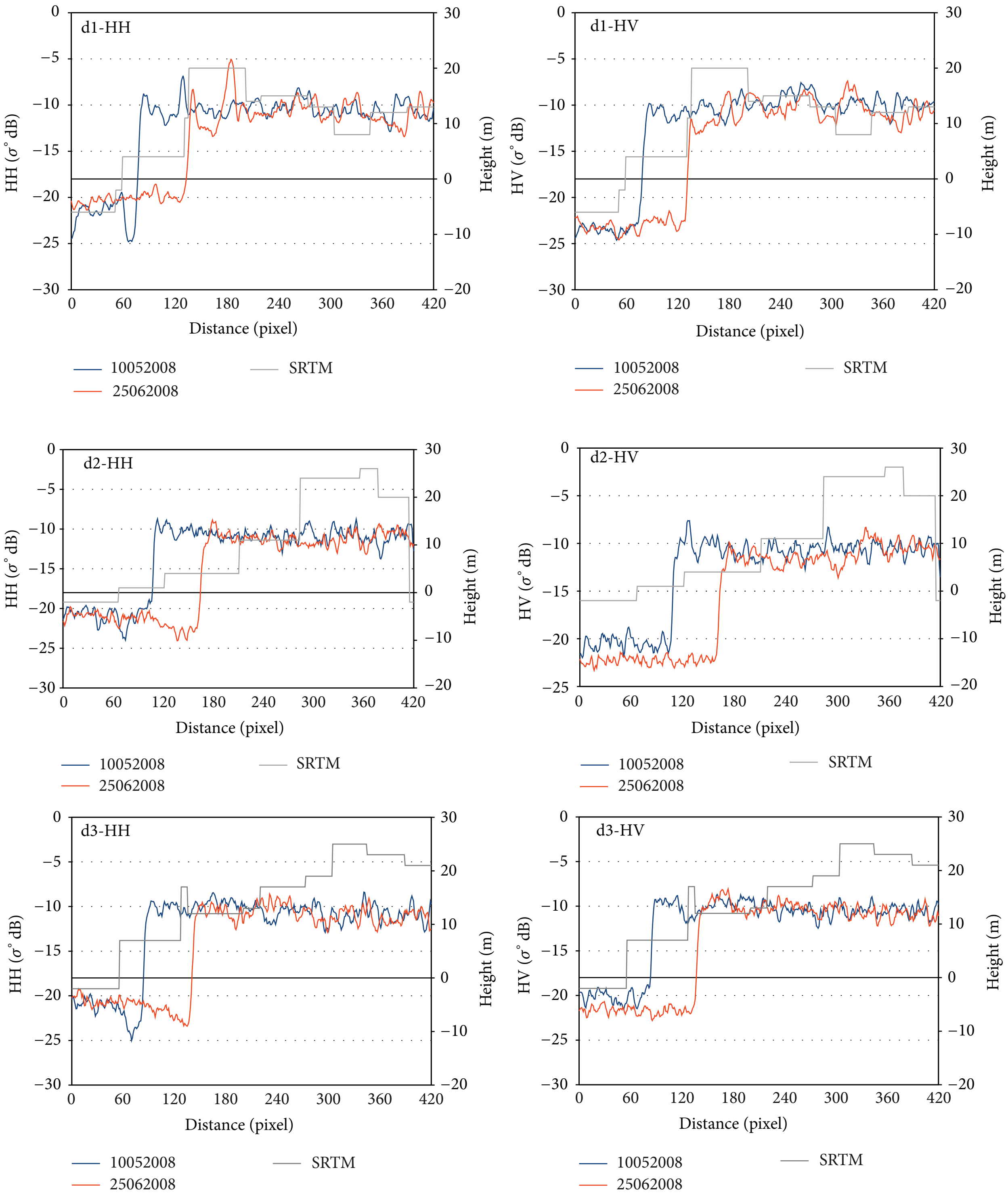

FIGURE 5: Impact of tidal height on ALOS PALSAR polarimetric measurement on HH and HV in Banyuasin, South Sumatera.

25-06-2008 when high tide occurred that high tide caused flooding of open zones, requiring ALOS PALSAR to penetrate more water on the underlying layer. In this situation, ALOS PALSAR radiation has specular reflection which produces backscatter value on HH and HV less on −20 dB. Meanwhile, the majority of area in the middle zone has backscatter value on HH and HV around −10 dB. This shows that on the middle zone, ALOS PALSAR penetrates mangrove areas and dry surface so its radiation has multiple and double bounce reflection.

4.2.2. Case Study in Cilacap Central Java. We used three ALOS PALSAR polarimetric measurements on HH and HV that covered mangrove forest at Cilacap, Central Java. The

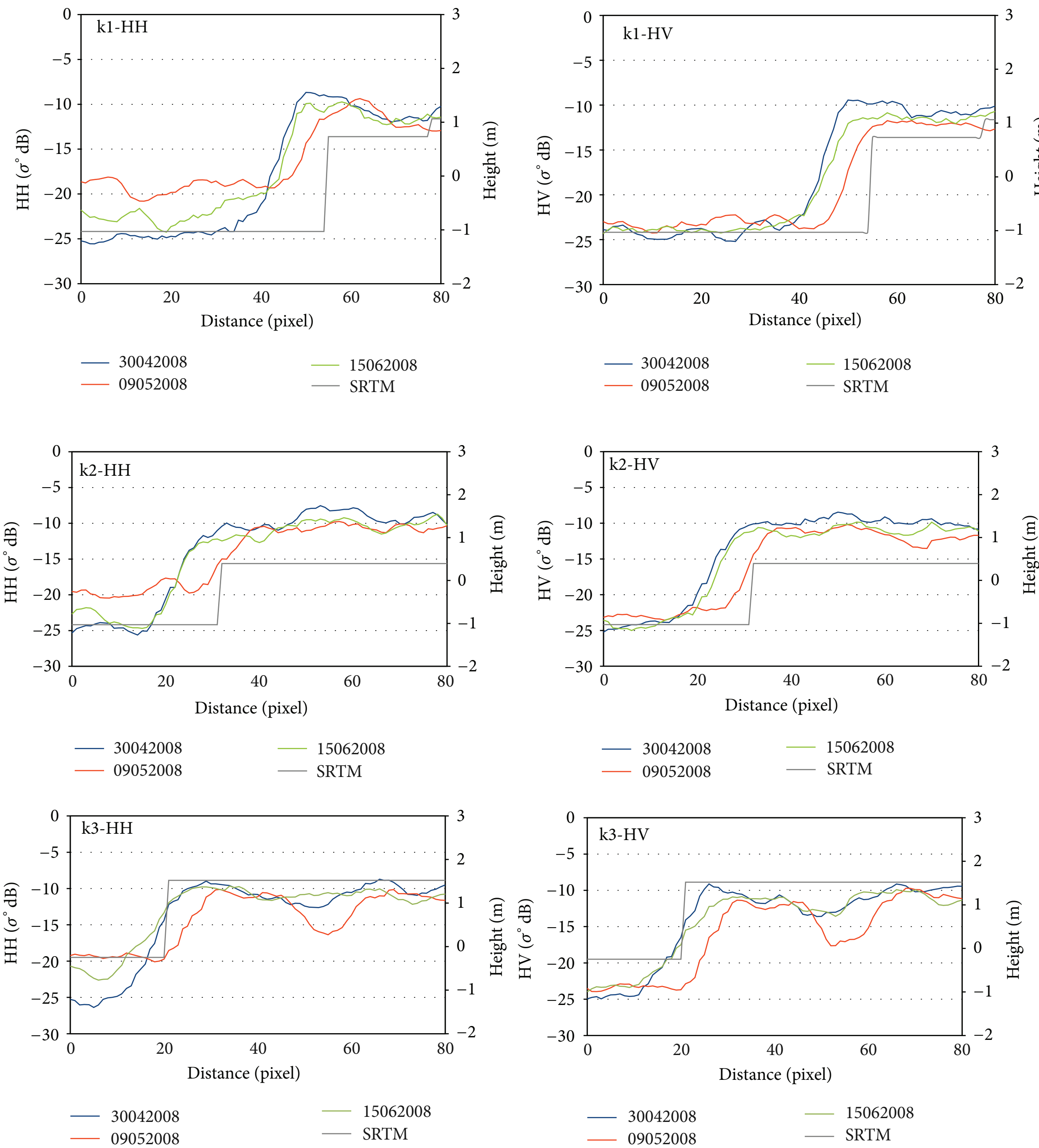

Figure 6: Impact of tidal height on ALOS PALSAR polarimetric measurement on HH and HV in Cilacap, Central Java.

first acquisition date was on 30-04-2008 at 15:33:49.697, the second on 09-05-2008 at 02:50:03.551, and the third on 15-06-2008 at 15:33:31.460. Each acquisition date has differences in tidal height. The measurement on acquisition date of 30-04-2008 at 15:33:49.697 showed tidal height around −0.4 meters, on 09-05-2008 at 02:50:03.551 tidal height around 1.0 meter, and on 09-05-2008 at 02:50:03.551 tidal height around −0.2 meter.

According to SRTM data, the level of topography on most of the mangrove zones in Cilacap is low and relatively flat, with 90% of the total areas having level of topography of less than 4 meters.

Figure 6 shows the impact of tidal height on ALOS PALSAR polarimetric measurement on HH and HV based on profiling as ROI with length of 80 pixels. The number 0 (zero) on the axis "distance on pixel" serves as a starting point for water areas. The water area (distance on pixel 0–40 at k1) showed a majority of backscatter value around −20 dB on HH and around −25 dB on HV. The water area has a wide variety of backscatter value on HH due to the waves, since HH polarimetric is more sensitive to water waves compared to HV polarimetric. The open zone has different backscatter pattern between the three acquisition dates, and these differences are caused by difference in tidal height. The measurement on 15-06-2008 has the highest tides, suggesting flooding on the open zone, thus causing ALOS PALSAR radiation to have specular reflection which produce backscatter value of less than −20 dB on HH and less than −25 dB on HV. The condition is quite different from the measurement with acquisition date of 30-04-2008 when a nonflooding situation occurred at the open zone. The measurement on 30-04-2008 produces backscatter value around −20 to −10 dB on HH and around −25 to −10 dB on HV.

At the middle zone, the measurement with acquisition date of 15-06-2008 has lower backscatter value, especially on HV. A comparison with acquisition dates 30-04-2008 and 09-05-2008 shows a deviation of −1.6 dB. This is due to the characteristics of mangrove zones in Cilacap area with their relatively flat topography, allowing high tides to cause flooding and mud surface. The underlying layer of mud surfaces or more water content will produce lower backscatter value compared to underlying layer of dry soil or sand. This indicates that backscatter value derived on ALOS PALSAR measurement on the mangrove zone is affected by underlying layer (e.g., tidal height and topography) and mangrove structure (e.g., leaf, branches, and trunks).

4.2.3. Case Study in Teluk Bintuni Papua. We used two ALOS PALSAR polarimetric measurements on HH and HV that cover mangrove forest in Teluk Bintuni, Papua. The first acquisition date was on 27-06-2008 at 13:51:32.107 and the second on 27-09-2008 at 13.52:53.001. Each acquisition date has differences of tidal height. Acquisition date on 27-09-2008 at 13.52:53.001 has higher tidal height compared to that of acquisition date on 27-06-2008 at 13.51:32.107. Based on SRTM data, the level of topography of the mangrove zone in Teluk Bintuni, Papua, is mostly high, with level of topography of less than 4 meters only covering 8% of total areas.

Figure 7 shows the impact of tidal height on ALOS PALSAR polarimetric measurement on HH and HV based on profiling as ROI with length of 140 pixels. The number 0 (zero) on the axis “distance on pixel” serves as a starting point for water areas. The water area (distance on pixel 0–50 at q1) shows a majority of backscatter value of less than −20 dB on HH and less than −25 dB on HV. The profiles q1 and q3 for the open zone show different backscatter pattern between acquisition date on 27-06-2008 and 27-09-2008, due to different tidal height. Acquisition date on 27-09-2008 has the highest tidal height, suggesting flooding at the open zone, thus causing ALOS PALSAR radiation to have specular reflection which produce backscatter value of less than −20 dB on HH and less than −25 dB on HV. The condition was quite different from acquisition date 27-06-2008 when a nonflooding situation occurred at the open zone. The acquisition date 27-06-2008 produce backscatter value around −20 to −10 dB on HH and around −25 to −10 dB on HV. On the middle zone, ALOS PALSAR penetrates mangrove areas and dry surface so ALOS PALSAR radiation has multiple and double bounce reflection.

4.3. Aboveground Biomass Estimation in Indonesia. Previous research on the characterization of mangrove forest in Indonesia [28] revealed the characteristics of mangrove forest based on ALOS PALSAR mosaics on the twenty sites of mangrove forest in Indonesia. Their sites covered a vast areas of mangrove forests, thus enabling them to describe all types of mangrove forest in overall Indonesia. The twenty sites of mangrove forest in Indonesia are (a) Langsa, Aceh, (b) Bengkalis, Riau, (c) Indragiri Hilir, Riau, (d) Banyuasin, South Sumatera, (e) Pontianak, West Kalimantan, (f) Kotabaru, South Kalimantan, (g) Kutai Kartanegara, East Kalimantan, (h) Berau, East Kalimantan, (i) Nunukan, East Kalimatan, (j) Subang, West Java, (k) Cilacap, Central Java, (l) Badung, Bali, (m) Bombana, Southeast Sulawesi, (n) Muna, Southeast Sulawesi, (o) Sorong, West Papua, (p) Teluk Bintuni, Papua, (q) Teluk Bintuni, Papua, (r) Waropen, Papua, (s) Asmat, Papua, and (t) Merauke Papua. Figures 8 and 9 show the characteristics of mean and standard deviation of backscatter coefficients on HH and HV for twenty Indonesian mangrove forests. From those figures, we can see that the mean for HH is around −10 dB to −7 dB, while the mean for HV is around −20 dB to −16 dB.

For estimations of AGB, some researchers [8, 10, 19] found empirical functions to estimate AGB, as derived from relationships between AGB measured on the ground sample plot and ALOS PALSAR polarimetric measurement, although using ALOS PALSAR for estimating AGB at regional level requires more detailed analysis [29]. In this study we have shown the impact of tidal height on ALOS PALSAR polarimetric measurement on HH and HV and we have estimated average AGB of mangrove forest at some area in Indonesia using algorithms 4, 5, and 6 and have the impact of tidal height and level of topography included in the calculation. Basically, the impact of tidal height on the open zones is quite significant, as can be seen from the variances of backscatter values. However, since the open zones only cover a diminutive area compared to the middle zones, this study shall focus on the latter. Based on the case of Cilacap, for the level of topography of less than 4 meters, with the size of mangrove zone impacted by tidal height which reached more than 90% of its total area, the backscatter value on HV has a deviation of −1.6 dB. However, to be able to calculate more accurately the deviation value caused by the impact of tidal height requires more time series ALOS PALSAR measurements and more tidal height data.

Table 2 shows the characteristics of level of topography, impact of tidal height on percentage of area, and the average of AGB estimation. The estimated averages of AGB in this study are within a reasonable range when compared with other studies which estimated an average of aboveground biomass in Aceh around 11.68 ton/ha, South Sumatera 43.72 ton/ha, and Riau 33.40 ton/ha [30], or in Malaysia around 2.98–378 ton/ha with an average of 99.40 ton/ha [19].

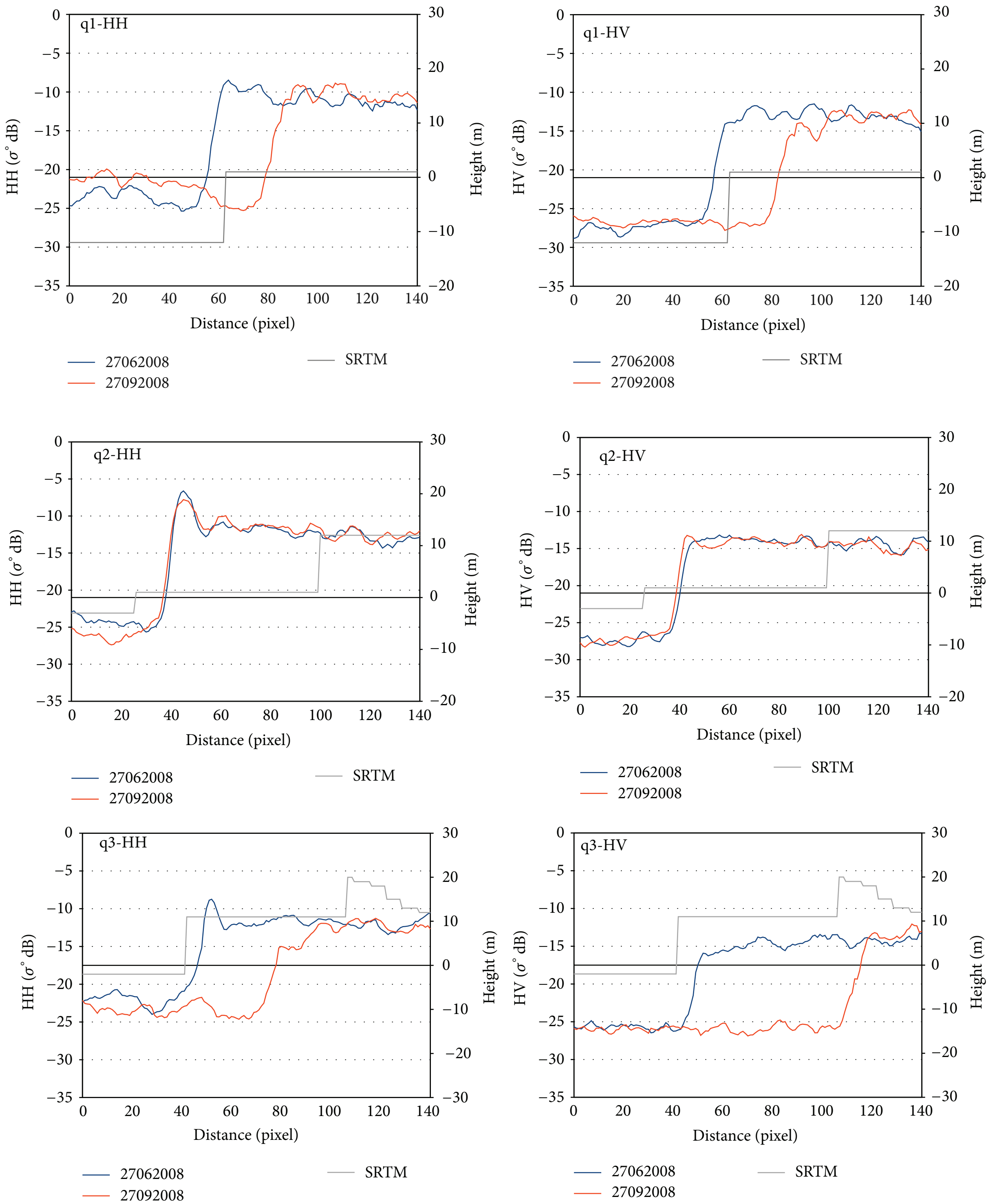

Figure 7: Impact of tidal height on ALOS PALSAR polarimetric measurement on HH and HV in Teluk Bintuni, Papua.

Table 2: Characteristics of topography, impact of tidal height on % area, and averages estimation of AGB mangroves forest in Indonesia.

Site	Location of mangrove zones	Average level of topography (meters)	Impact of tidal height (on % area)	Averages AGB estimation (ton/ha)
a	Langsa Aceh	2.2 ± 5.4	95	1.57–20.65
b	Bengkalis Riau	4.9 ± 1.9	40	26.08
c	Indragiri hilir Riau	6.8 ± 4.7	4	14.64
d	Banyuasin South Sumatera	16.8 ± 4.9	4	26.68
e	Pontianak West Kalimantan	10.2 ± 3.3	4	18.76
f	Kota Baru South Kalimantan	9.5 ± 5.9	6	62.57
g	Kutai Kartanegara East Kalimantan	9.6 ± 4.8	6	47.59
h	Berau East Kalimantan	15.0 ± 5.4	4	31.38
i	Nunukan East Kalimantan	14.5 ± 3.4	4	32.51
j	Subang West Java	3.0 ± 1.8	95	0.83–4.38
k	Cilacap Central Java	2.9 ± 2.1	90	1.70–19.36
l	Badung Bali	3.1 ± 2.0	73	3.47–85.56
m	Bombana South Sulawesi	8.8 ± 4.4	18	24.92
n	Muna South Sulawesi	10.6 ± 3.8	10	77.78
o	Sorong Papua	13.4 ± 4.5	5	85.76
p	Teluk Bintuni Papua	19.9 ± 11.2	6	17.79
q	Teluk Bintuni Papua	18.7 ± 8.3	4	23.30
r	Waropen Papua	19.3 ± 4.3	2	57.79
s	Asmat Papua	14.8 ± 3.5	2	23.30
t	Merauke Papua	11.7 ± 3.4	2	3.97

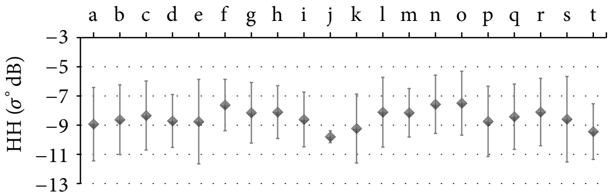

Figure 8: Mean and standard deviation of backscatter coefficients on HH.

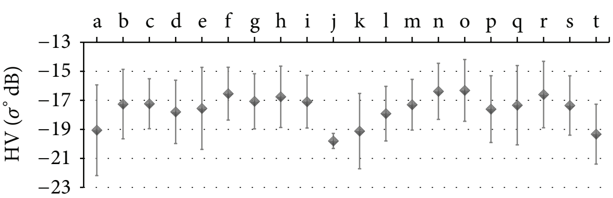

Figure 9: Mean and standard deviation of backscatter coefficients on HV.

5. Conclusion

This study showed a variety of tidal heights and levels of topography that cause distribution of flooding and nonflooding area at open and middle zones of mangrove forests. The open zones are highly impacted by tidal height, as evident by the flood that often occurs during high tides, whereas the middle zones experienced no significant impact of tidal height as evident by the occurrence of nonflooding area on most of its zone.

Based on ALOS PALSAR polarimetric measurement on HH and HV, flooding and nonflooding areas on the mangrove zones produce unique characteristics of backscatter value. These characteristics are the combined product of the effect of tidal height and the level of topography of the area. For the open zones, the backscatter during high tide in flooded areas showed values of less than −20 dB on HH and less than −25 dB on HV, except in Banyuasin where HV values are less than −20 dB. On the other hand, low tide and nonflooding produce a backscatter value around −20 to −10 dB on HH and around −25 to −10 dB on HV, except in Banyuasin with HV value from −20 to −10 dB.

At the middle zones, high topography and the variety of tidal height in Banyuasin and Teluk Bintuni produce similar backscatter value, unlike those of Cilacap with its low and flat topography that showed a 1.6 dB deviation of backscatter value on HV.

Differences in backscatter values of the open zones and deviation of backscatter values of the middle zone can be used to enhance and to improve algorithm model for estimating AGB mangrove forest based on ALOS PALSAR measurements, although it is agreed that the degree of accuracy of the estimation depends on the number of time series ALOS PALSAR measurements and tidal height data. Within the acknowledged limitation of this study, the different impact of tidal height on the backscatter value of HH and HV for different zone of mangrove forests has been demonstrated and used to estimate AGB mangrove forest in Indonesia. Based on ALOS PALSAR measurement that had included the impact of topography and tidal height, mangrove zones in Subang West Java have the smallest value of AGB with an average value of 0.83–4.38 ton/ha, while Sorong Papua has the largest value of AGB with an average value of 85.76 ton/ha.

Conflict of Interests

The authors declare that there is no conflict of interests regarding the publication of this paper.

Acknowledgments

This study is carried out as a JAXA SAFE Project. The author would like to thank JAXA for their support.

References

[1] P. B. Tomlinson, *The Botany of Mangroves*, Cambridge University Press, Cambridge, UK, 1986.

[2] G. M. Wightman, "Mangroves of the northern territory," Northern Territory Botanical Bulletin no. 7, Conservation Commission of The Northern Territory, Palmerstone, Australia, 1989.

[3] W. Giesen, S. Wulffraat, M. Zieren, and L. Scholten, *Mangrove Guidebook for South East Asia*, FAO, Wetlands International, Bangkok, Thailand, 2007.

[4] C. Kuenzer, A. Bluemel, S. Gebhardt, T. V. Quoc, and S. Dech, "Remote sensing of mangrove ecosystems: a review," *Remote Sensing*, vol. 3, no. 5, pp. 878–928, 2011.

[5] C. Nellemann, E. Corcoran, C. M. Duarte, L. Valdes, C. de Young, and L. Fonseca, *Blue Carbon, A Rapid Response Assessment*, United Nations Environment Programme, Arendal, Norway, 2009.

[6] D. C. Donato, J. B. Kauffman, D. Murdiyarso, S. Kurnianto, M. Stidham, and M. Kanninen, "Mangroves among the most carbon-rich forests in the tropics," *Nature Geoscience*, vol. 4, no. 5, pp. 293–297, 2011.

[7] Y. R. Noor, M. Khazali, and I. N. N. Suryadiputra, *Panduan Pengenalan Mangrove di Indonesia. PHKA/WI-IP*, Wetlands International, Bogor, Indonesia, 1999.

[8] W. Takeuchi, D. V. Tien, V. T. Phuong, A. N. Van, and K. S. Oo, "Above ground biomass mapping of mangrove forest in Vietnam by ALOS PALSAR," in *Proceedings of the 3rd International Asia-Pacific Conference on Synthetic Aperture Radar (APSAR '11)*, pp. 1–3, IEEE, Seoul, South Korea, September 2011.

[9] F. M. Henderson and A. J. Lewis, "Radar detection of wetland ecosystems: a review," *International Journal of Remote Sensing*, vol. 29, no. 20, pp. 5809–5835, 2008.

[10] R. M. Lucas, A. L. Mitchell, A. Rosenqvist, C. Proisy, A. Melius, and C. Ticehurst, "The potential of L-band SAR for quantifying mangrove characteristics and change: case studies from the tropics," *Aquatic Conservation: Marine and Freshwater Ecosystems*, vol. 17, no. 3, pp. 245–264, 2007.

[11] R. Tsolmon, R. Tateishi, and J. S. S. Tetuko, "A method to estimate forest biomass and its application to monitor Mongolian Taiga using JERS-1 SAR data," *International Journal of Remote Sensing*, vol. 23, no. 22, pp. 4971–4978, 2002.

[12] R. M. Lucas, M. Moghaddam, and N. Cronin, "Microwave scattering from mixed-species forests, Queensland, Australia," *IEEE Transactions on Geoscience and Remote Sensing*, vol. 42, no. 10, pp. 2142–2159, 2004.

[13] K. O. Pope, J. M. Rey-Benayas, and J. F. Paris, "Radar remote sensing of forest and wetland ecosystems in the Central American tropics," *Remote Sensing of Environment*, vol. 48, no. 2, pp. 205–219, 1994.

[14] Y. Wang, L. L. Hess, S. Filoso, and J. M. Melack, "Understanding the radar backscattering from flooded and nonflooded Amazonian forests: results from canopy backscatter modeling," *Remote Sensing of Environment*, vol. 54, no. 3, pp. 324–332, 1995.

[15] P. Townsend, "Relationships between forest structure and the detection of flood inundation in forested wetland using C-band SAR," *International Journal of Remote Sensing*, vol. 22, pp. 443–460, 2001.

[16] P. A. Townsend, "Mapping seasonal flooding in forested wetlands using multi-temporal Radarsat SAR," *Photogrammetric Engineering and Remote Sensing*, vol. 67, no. 7, pp. 857–864, 2001.

[17] C. Proisy, E. Mougin, F. Fromard, V. Trichon, and M. A. Karam, "On the influence of canopy structure on the radar backscattering of mangrove forests," *International Journal of Remote Sensing*, vol. 23, no. 20, pp. 4197–4210, 2002.

[18] A. C. Morel, S. S. Saatchi, Y. Malhi et al., "Estimating aboveground biomass in forest and oil palm plantation in Sabah, Malaysian Borneo using ALOS PALSAR data," *Forest Ecology and Management*, vol. 262, no. 9, pp. 1786–1798, 2011.

[19] O. Hamdan, H. Khali Aziz, and I. Mohd Hasmadi, "L-band ALOS PALSAR for biomass estimation of Matang Mangroves, Malaysia," *Remote Sensing of Environment*, vol. 155, pp. 69–78, 2014.

[20] M. L. Imhoff, "A theoretical analysis of the effect of forest structure on synthetic aperture radar backscatter and the remote sensing of biomass," *IEEE Transactions on Geoscience and Remote Sensing*, vol. 33, no. 2, pp. 341–352, 1995.

[21] M. Shimada, O. Isoguchi, T. Tadono, and K. Isono, "PALSAR radiometric and geometric calibration," *IEEE Transactions on Geoscience and Remote Sensing*, vol. 47, no. 12, pp. 3915–3932, 2009.

[22] L. M. Varnell, D. A. Evans, and K. J. Havens, "A geomorphological model of intertidal cove marshes with application to wetlands management," *Ecological Engineering*, vol. 19, no. 5, pp. 339–347, 2003.

[23] E. Wolanski, "Hydrodynamics of mangrove swamps and their coastal waters," *Hydrobiologia*, vol. 247, no. 1–3, pp. 141–161, 1992.

[24] Y. Mazda, D. Kobashi, and S. Okada, "Tidal-scale hydrodynamics within mangrove swamps," *Wetlands Ecology and Management*, vol. 13, no. 6, pp. 647–655, 2005.

[25] J. M. Knight, P. E. R. Dale, R. J. K. Dunn, G. J. Broadbent, and C. J. Lemckert, "Patterns of tidal flooding within a mangrove forest: coombabah Lake, Southeast Queensland, Australia," *Estuarine, Coastal and Shelf Science*, vol. 76, no. 3, pp. 580–593, 2008.

[26] E. Rodríguez, C. S. Morris, J. E. Belz et al., "An Assessment of the SRTM Topographic Products," http://www2.jpl.nasa.gov/srtm/SRTM_D31639.pdf.

[27] F. Darboux, P. Davy, C. Gascuel-Odoux, and C. Huang, "Evolution of soil surface roughness and flowpath connectivity in overland flow experiments," *Catena*, vol. 46, no. 2-3, pp. 125–139, 2002.

[28] S. Darmawan, W. Takeuchi, Y. Vetrita, K. Wikantika, and D. Sari, "Characterization of mangrove forest types based on ALOS-PALSAR in overall Indonesian archipelago," *IOP Conference Series: Earth and Environmental Science*, vol. 20, Article ID 012051, 2014.

[29] R. Lucas, J. Armston, R. Fairfax et al., "An evaluation of the ALOS PALSAR L-band backscatter—above ground biomass relationship Queensland, Australia: impacts of surface moisture condition and vegetation structure," *IEEE Journal of Selected Topics in Applied Earth Observations and Remote Sensing*, vol. 3, no. 4, pp. 576–593, 2010.

[30] D. M. Yuwono, S. W. Wijaya, T. Hidayatullah, P. Meissarah, E. Prahasta, and I. Hayatiningsih, *Pemetaan Mangrove Sumatera, Provinsi Aceh, Sumatera Utara dan Riau*, Badan Infromasi Geospasial (BIG), Bogor, Indonesia, 2013.